

UC Davis

UC Davis Previously Published Works

Title

A Novel Population of Wake-Promoting GABAergic Neurons in the Ventral Lateral Hypothalamus.

Permalink

<https://escholarship.org/uc/item/3j38c9g1>

Journal

Current biology : CB, 26(16)

ISSN

0960-9822

Authors

Venner, Anne
Anaclet, Christelle
Broadhurst, Rebecca Y
et al.

Publication Date

2016-08-01

DOI

10.1016/j.cub.2016.05.078

Peer reviewed



HHS Public Access

Author manuscript

Curr Biol. Author manuscript; available in PMC 2017 August 22.

Published in final edited form as:

Curr Biol. 2016 August 22; 26(16): 2137–2143. doi:10.1016/j.cub.2016.05.078.

A novel population of wake-promoting GABAergic neurons in the ventral lateral hypothalamus

Anne Venner, Christelle Anaclet, Rebecca Y. Broadhurst, Clifford B. Saper, and Patrick M. Fuller

Department of Neurology, Beth Israel Deaconess Medical Center, Boston, MA 02215. Division of Sleep Medicine, Harvard Medical School, Boston, MA 02115

Summary

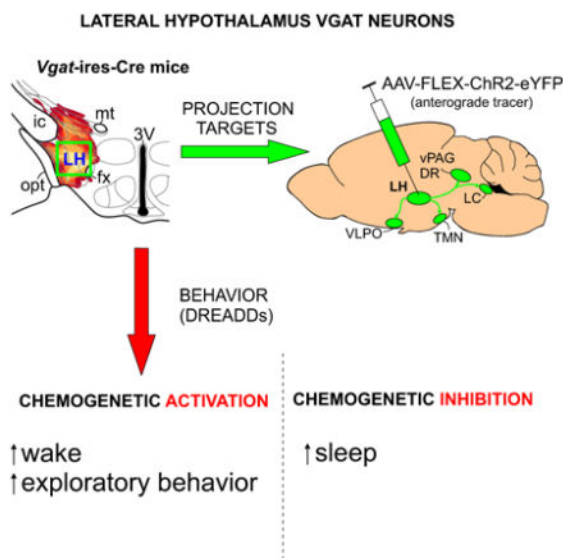
The largest synaptic input to the sleep-promoting ventrolateral preoptic area (VLPO) [1] arises from the lateral hypothalamus [2], a brain area associated with arousal [3–5]. However, the neurochemical identity of the majority of these VLPO-projecting neurons within the LH, as well as their function in the arousal network, remains unknown. Herein we describe a population of VLPO-projecting neurons in the LH that express the vesicular GABA transporter (VGAT; a marker for GABA-releasing neurons). In addition to the VLPO, these neurons also project to several other established sleep and arousal nodes, including the tuberomammillary nucleus, ventral periaqueductal gray and locus coeruleus. Selective and acute chemogenetic activation of LH VGAT+ neurons was profoundly wake-promoting whereas acute inhibition increased sleep. Because of its direct and massive inputs to the VLPO, this population may play a particularly important role in wake-sleep switching.

Graphical abstract

Contact: pfuller@bidmc.harvard.edu.

Author Contributions: AV, CBS and PMF conceived of the experiments. AV, CA and RYB performed the experiments and analyzed the data. AV, CA, RYB, CBS and PMF interpreted the data and wrote the paper.

Publisher's Disclaimer: This is a PDF file of an unedited manuscript that has been accepted for publication. As a service to our customers we are providing this early version of the manuscript. The manuscript will undergo copyediting, typesetting, and review of the resulting proof before it is published in its final citable form. Please note that during the production process errors may be discovered which could affect the content, and all legal disclaimers that apply to the journal pertain.



RESULTS

Previous work has shown that the LH is the largest single source of neurons retrogradely labeled from the VLPO, but only about 4% of these neurons contain the peptide orexin and 21% contain melanin-concentrating hormone (MCH) [2]. Since lateral hypothalamic lesions generally cause sleepiness [5], we hypothesized that the neurons that innervate the VLPO may be inhibitory, and play an important role in sleep regulation. To determine whether the LH neurons that innervate the VLPO contain GABA, we first placed unilateral injections of an adeno-associated viral (AAV) vector EF1a-FLEX-hChR2 (H134R)-eYFP-AAV10 into the ventral two-thirds of the LH (Figure 1A) at the level of the ventromedial nucleus in *Vgat-IRES-cre* mice (Figure 1B1). Importantly, VGAT⁺ neurons expressing ChR2-YFP (ChR2-eYFP⁺) are distinct from the neighboring orexin and MCH neurons [6–10] (Figure 1B2–3). Histological evaluation of the terminal fields of LH VGAT⁺ neurons revealed a dense ChR2-eYFP⁺ projection to the VLPO (Figure 1C) and several other brain areas involved in sleep-wake control, specifically the tuberomammillary nucleus (TMN) [11, 12], locus coeruleus (LC) [13, 14], ventral periaqueducal gray (VPAG) [15] and parabrachial nucleus (PB) [16] (Figure 1D–F). ChR2-eYFP⁺ fibers were densely clustered around histidine decarboxylase (HDC)-containing neurons in the TMN and, to a lesser extent, serotonergic (5-HT) neurons in the dorsal raphe (DR) and tyrosine hydroxylase (TH)-containing neurons in the VPAG and LC (Figure [S1]). Notably, axonal labelling was relatively sparse in the sleep-promoting parafacial zone (PZ) [17, 18] and completely absent throughout the thalamic reticular nucleus (RTN) [19] (Figure 1G–I), the latter of which receives inputs from both from the dorsally adjacent zona incerta and the rostrally and laterally adjacent basal forebrain [20].

We next determined the functional role of LH VGAT⁺ neurons in arousal control via conditional chemogenetic activation of LH VGAT⁺ neurons, using the excitatory Designer Receptor Exclusively Activated by a Designer Drug (DREADD; AAV-hSyn-DIO-hM3Dq-

mCherry, henceforth: AAV-hM3Dq). We specifically placed injections of AAV-hM3Dq into the ventral 2/3 of the LH at the level of the ventromedial nucleus in Vgat-IRES-cre mice (Figure 2A) and confirmed in vivo cellular activation of hM3Dq+ LH neurons by the hM3Dq ligand, clozapine-N-oxide (CNO; IP, 0.3mg/kg; Figure 2B). Following CNO and vehicle (saline) injection, mice were monitored for sleep-wake and their arousal state was scored based upon both EEG and EMG signals.

Injections of CNO at 10AM - a time approximating peak sleep drive in the mouse - produced uninterrupted wake that lasted 4–6 hours, along with a concomitant reduction in NREM and REM sleep (Figure 2C). During the early night period following CNO-induced wakefulness a prominent quantitative sleep rebound was observed (Figure 2C, [S2]), but waking levels were normalized by the next day. Activation of LH VGAT+ neurons also markedly increased high theta (6–10 Hz) and high gamma (70–200Hz) band EEG power - two frequency domains associated with active wakefulness [21] (Figure 2D).

Immediately following the CNO-induced waking period, there was a rebound increase in delta power (0.5–4 Hz) during NREM that was qualitatively comparable to that following a period of sleep deprivation by gentle handling in this strain of mice (Figure [S2]). Furthermore, there was a period of quantitative sleep rebound (increased NREM and REM, Figure 2C) between 8PM and 11PM, during which time a small reduction in waking theta and gamma was observed (Figure [S2]). Administration of CNO at 7PM - a time of high waking drive in the mouse - produced a longer waking response than was seen following 10AM injections and increased high theta and beta band (12–20Hz) EEG power but, interestingly, did not elicit a sleep rebound (Figure [S2]).

To determine whether the animals exhibited typical waking behaviors during the CNO-induced waking state, we employed a video-based behavioral analysis and scored each 4 second epoch of behavior into categories. When CNO-induced waking behaviors were compared with those observed during the early night period (when mice are most active), CNO-activated mice spent significantly more time foraging and exploring the bottom of their cage, at the expense of grooming or climbing/rearing. There was no difference in the amount of time CNO-activated mice spent eating, drinking or ambulating (in the absence of foraging/digging or climbing/rearing) compared with controls (Figure 2E).

We next examined and quantified c-Fos activity following administration of CNO at 10AM in selected putative downstream targets of the hM3Dq+ LH VGAT+ neurons (e.g., VLPO, TMN and LC). The number of c-Fos+ neurons in the sleep-promoting VLPO was significantly decreased in mice treated with CNO compared with saline. The number of c-Fos+ neurons in the LC and TMN did not differ between the two conditions, which was a surprising finding given the dense LH VGAT+ axonal field in these brain regions (Figure 2F).

To more precisely define the anatomical region of LH VGAT+ neurons whose activation drives behavioral and EEG wake, we placed very small unilateral injections of AAV-hM3Dq in and around the perifornical LH in Vgat-IRES-cre mice and recorded sleep-wake following saline and CNO injections. Mice were designated as phenotypic if their percent

wakefulness between 1–2 hours following CNO administration was over 1 standard deviation above the mean of the vehicle injection during the same time period (i.e. a Z score greater than 1). Following behavioral experiments, the mice were sacrificed and their brains processed for immunolabelling against mCherry. For each phenotypic mouse, we projected the extent of the transduced neurons (comprising hM3Dq-mCherry+ somata) onto a series of standard sections and thereby constructed a heat map, showing overlapping sites of hM3Dq+ neurons from different mice (Figure 2G). From this, we inferred a delimited node of LH VGAT+ neurons responsible for mediating the waking phenotype, which comprised neurons lateral to the fornix, ventral to ZI, medial to the optic nerve and centered at bregma –1.7. Mice bearing hM3Dq-mCherry+ neurons outside of this node, for example confined to the zona incerta or medial to the fornix, did not exhibit increased wakefulness following CNO injection (Figure [S3]).

We lastly placed injections of the inhibitory DREADD, hM4Di (AAV-hSyn-hM4Di-mCherry) into our delimited node in Vgat-IRES-cre mice (Figure 3A) to determine the effects of acute inhibition of these VGAT+ neurons on wake. Absence of c-Fos immunoreactivity in hM4Di+ LH neurons following CNO administration (i.p.) indicated that the cells were in a lower state of neuronal activation, particularly when compared against activated neurons in mice injected with hM3Dq (cf Figure 3B2 and Figure 2B2). Administration of CNO at 7pm resulted in a cumulative ~15% (35 minutes) reduction in wake and a concomitant ~60% (35 minutes) increase in NREM sleep over the 3-hour post injection period, while REM sleep quantity remained unchanged (Figure 3C). In addition, analysis of the EEG evidenced a reduction of high theta power during waking (Figure 3D) while VGAT+ neurons were inhibited, establishing necessity of these neurons for both normal levels of behavioral wake and a normal waking EEG.

DISCUSSION

Our results show that LH VGAT+ neurons 1) send a dense putatively inhibitory projection to several brain regions associated with sleep and arousal control, and 2) are potently wake promoting.

A current model of arousal regulation in the mammal is the ‘flip-flop’ switch [22]. The basic principle of the model is that brain regions involved in promoting sleep (e.g. VLPO) and wake (TMN, LC, LH, vPAG) act in opposition to each other, largely through mutual inhibitory connections. At the same time, these circuits are also under the control of circadian, homeostatic and allostatic influences [22]. These factors determine when the state of reciprocal inhibition between the sleep- and wake-promoting nodes is switched, thereby resulting in a change in arousal state. Mathematical modeling based on this hypothesis has been shown to reproduce not only wake-sleep dynamics in a variety of species, but also in various diseases [23, 24]. The wake-promoting LH VGAT+ neurons described herein project heavily to the VLPO and are thus well-placed to inhibit sleep-promoting neurons, thereby favoring the wake state. The reduction in VLPO c-Fos expression following hM3Dq activation of LH VGAT+ neurons with CNO provides some support for this concept, although additional experiments, including terminal inhibition, will be required to confirm this possibility. VLPO axons also project extensively to the LH[11] suggesting that LH

VGAT+ neurons may play an important role in the flip-flop switch. Surprisingly, (considering their wake promoting phenotype), LH VGAT+ neurons also project heavily to the wake-promoting LC, TMN and vPAG. It is not immediately clear how an inhibitory projection would activate wake-promoting neurons, although one, as yet untested, possibility is through disinhibition of inhibitory interneurons/axons in the target regions. It is of interest to note that our delimited node of LH VGAT+ neurons project relatively sparsely to the sleep-promoting PZ [17, 18] and not at all to the RTN [19], so it is unlikely that they elicit their wake-promoting effects via either of these circuits. Our conditional tracing also reveals that the downstream targets of the LH VGAT+ neurons are quite distinct from those of the more rostrally-situated wake-promoting VGAT+ basal forebrain [25] which do not project to the VLPO, but do project to the RTN. The wake-promoting LH VGAT+ neurons identified in the present study are therefore clearly not an anatomic or functional continuum of basal forebrain GABAergic neurons.

Similarly, although a recent study has reported that the RTN receives a GABA-ergic input from the LH that is also wake-promoting [19], (consistent with earlier tracer work describing a projection from the dorsal LH, in or near the zona incerta, to the RTN [20]), anterograde tracing from the node of anatomically defined ventral LH VGAT+ neurons in the present study did not reveal a projection to the RTN. Hence, the wake-promoting LH VGAT+ neurons described herein must comprise a separate and distinct population from the cells that project to the RTN, and the wake promoting effects of acute activation would therefore likely involve downstream targets other than RTN, such as the VLPO.

In conclusion, we have identified an anatomical subpopulation of LH VGAT+ neurons whose activation potently drives wake and inhibition increases sleep. Furthermore, their projection pattern indicates that these neurons target several brain regions critical for mediating arousal states, including the sleep-promoting VLPO and, as such, are likely to represent an important circuit element of the ‘flip-flop’ switch [22].

Supplementary Material

Refer to Web version on PubMed Central for supplementary material.

Acknowledgments

We are grateful to Quan Ha, Minh Ha and Myriam Debruyne for superb technical assistance. We are also indebted to Drs. Bradford Lowell and Linh Vong for supplying us with the breeder pairs for developing our Vgat-IRES-cre line of mice. This work was supported by a NARSAD Young Investigator grant from the Brain & Behavior Research Foundation (AV), National Institutes of Health grants NS073613 and NS092652 (PMF), NS085477 (CBS) and the G. Harold and Leila Y. Mathers Foundation (CBS).

References

1. Sherin JE, Shiromani PJ, McCarley RW, Saper CB. Activation of Ventrolateral Preoptic Neurons During Sleep. *Science*. 1996; 271:216–219. [PubMed: 8539624]
2. Chou TC, Bjorkum AA, Gaus SE, Lu J, Scammell TE, Saper CB. Afferents to the Ventrolateral Preoptic Nucleus. *J Neurosci*. 2002; 22:977–990. [PubMed: 11826126]

3. Cerri M, Vecchio FD, Mastrotto M, Luppi M, Martelli D, Perez E, Tupone D, Zamboni G, Amici R. Enhanced Slow-Wave EEG Activity and Thermoregulatory Impairment following the Inhibition of the Lateral Hypothalamus in the Rat. *PLoS ONE*. 2014; 9:e112849. [PubMed: 25398141]
4. Clément O, Sapin E, Libourel PA, Arthaud S, Brischoux F, Fort P, Luppi PH. The Lateral Hypothalamic Area Controls Paradoxical (REM) Sleep by Means of Descending Projections to Brainstem GABAergic Neurons. *J Neurosci*. 2012; 32:16763–16774. [PubMed: 23175830]
5. Gerashchenko D, Kohls MD, Greco M, Waleh NS, Salin-Pascual R, Kilduff TS, Lappi DA, Shiromani PJ. Hypocretin-2-Saporin Lesions of the Lateral Hypothalamus Produce Narcoleptic-Like Sleep Behavior in the Rat. *J Neurosci*. 2001; 21:7273–7283. [PubMed: 11549737]
6. Jogo S, Glasgow SD, Herrera CG, Ekstrand M, Reed SJ, Boyce R, Friedman J, Burdakov D, Adamantidis AR. Optogenetic identification of a rapid eye movement sleep modulatory circuit in the hypothalamus. *Nat Neurosci*. 2013; 16:1637–1643. [PubMed: 24056699]
7. Konadhode RR, Pelluru D, Blanco-Centurion C, Zayachkivsky A, Liu M, Uhde T, Glen WB, van den Pol AN, Mulholland PJ, Shiromani PJ. Optogenetic Stimulation of MCH Neurons Increases Sleep. *J Neurosci*. 2013; 33:10257–10263. [PubMed: 23785141]
8. Adamantidis AR, Zhang F, Aravanis AM, Deisseroth K, de Lecea L. Neural substrates of awakening probed with optogenetic control of hypocretin neurons. *Nature*. 2007; 450:420–424. [PubMed: 17943086]
9. Tsunematsu T, Ueno T, Tabuchi S, Inutsuka A, Tanaka KF, Hasuwa H, Kilduff TS, Terao A, Yamanaka A. Optogenetic Manipulation of Activity and Temporally Controlled Cell-Specific Ablation Reveal a Role for MCH Neurons in Sleep/Wake Regulation. *J Neurosci*. 2014; 34:6896–6909. [PubMed: 24828644]
10. Chemelli RM, Willie JT, Sinton CM, Elmquist JK, Scammell T, Lee C, Richardson JA, Williams SC, Xiong Y, Kisanuki Y, et al. Narcolepsy in orexin Knockout Mice: Molecular Genetics of Sleep Regulation. *Cell*. 1999; 98:437–451. [PubMed: 10481909]
11. Sherin JE, Elmquist JK, Torrealba F, Saper CB. Innervation of Histaminergic Tuberomammillary Neurons by GABAergic and Galaninergic Neurons in the Ventrolateral Preoptic Nucleus of the Rat. *J Neurosci*. 1998; 18:4705–4721. [PubMed: 9614245]
12. Takahashi K, Lin JS, Sakai K. Neuronal Activity of Histaminergic Tuberomammillary Neurons During Wake–Sleep States in the Mouse. *J Neurosci*. 2006; 26:10292–10298. [PubMed: 17021184]
13. Carter ME, Brill J, Bonnavion P, Huguenard JR, Huerta R, de Lecea L. Mechanism for Hypocretin-mediated sleep-to-wake transitions. *PNAS*. 2012; 109:E2635–E2644. [PubMed: 22955882]
14. Carter ME, Yizhar O, Chikahisa S, Nguyen H, Adamantidis A, Nishino S, Deisseroth K, de Lecea L. Tuning arousal with optogenetic modulation of locus coeruleus neurons. *Nat Neurosci*. 2010; 13:1526–1533. [PubMed: 21037585]
15. Lu J, Zhou TC, Saper CB. Identification of Wake-Active Dopaminergic Neurons in the Ventral Periaqueductal Gray Matter. *J Neurosci*. 2006; 26:193–202. [PubMed: 16399687]
16. Fuller P, Sherman D, Pedersen NP, Saper CB, Lu J. Reassessment of the structural basis of the ascending arousal system. *J Comp Neurol*. 2011; 519:933–956. [PubMed: 21280045]
17. Anaclet C, Ferrari L, Arrigoni E, Bass CE, Saper CB, Lu J, Fuller PM. The GABAergic parafacial zone is a medullary slow wave sleep-promoting center. *Nat Neurosci*. 2014; 17:1217–1224. [PubMed: 25129078]
18. Anaclet C, Lin JS, Vetrivelan R, Krenzer M, Vong L, Fuller PM, Lu J. Identification and characterization of a sleep-active cell group in the rostral medullary brainstem. *J Neurosci*. 2012; 32:17970–17976. [PubMed: 23238713]
19. Herrera CG, Cadavieco MC, Jogo S, Ponomarenko A, Korotkova T, Adamantidis A. Hypothalamic feedforward inhibition of thalamocortical network controls arousal and consciousness. *Nat Neurosci*. 2016; 19:290–298. [PubMed: 26691833]
20. Hallanger AE, Levey AI, Lee HJ, Rye DB, Wainer BH. The origins of cholinergic and other subcortical afferents to the thalamus in the rat. *J Comp Neurol*. 1987; 262:105–124. [PubMed: 2442206]
21. O’Keefe J, Recce ML. Phase relationship between hippocampal place units and the EEG theta rhythm. *Hippocampus*. 1993; 3:317–330. [PubMed: 8353611]

22. Saper CB, Fuller PM, Pedersen NP, Lu J, Scammell TE. Sleep State Switching. *Neuron*. 2010; 68:1023–1042. [PubMed: 21172606]
23. Rempe MJ, Best J, Terman D. A mathematical model of the sleep/wake cycle. *J Math Biol*. 2009; 60:615–644. [PubMed: 19557415]
24. Behn CD, Brown EN, Scammell TE, Kopell N. A mathematical model of network dynamics governing sleep-wake patterns in mice. *J Neurophysiol*. 2007; 97:3828–3840. [PubMed: 17409167]
25. Anacleto C, Pedersen NP, Ferrari LL, Venner A, Bass CE, Arrigoni E, Fuller PM. Basal forebrain control of wakefulness and cortical rhythms. *Nat Comms*. 2015; 6:8744.

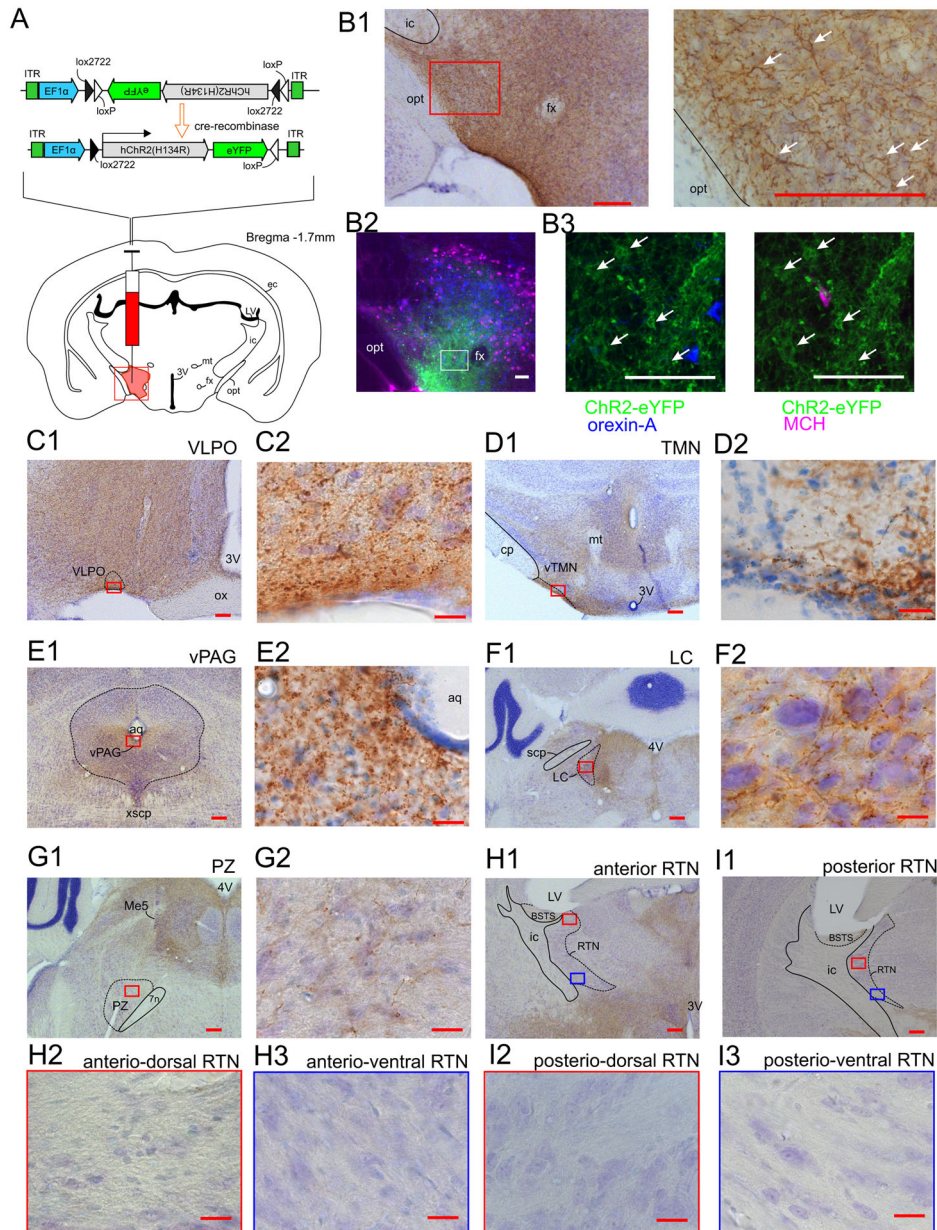


Figure 1. Conditional anterograde tracing from LH VGAT+ neurons

A) Schema of ChR2-eYFP construct and viral targeting to the LH of VGAT-ires-Cre mice. B1) Immunolabelling for eYFP (brown) in cell bodies in the LH, counterstained with Nissl (blue), arrows indicate ChR2-eYFP cell bodies. Scale: 200 μ m. B2) Low magnification photomicrograph indicating injection site of ChR2-eYFP (green) in a LH brain section immunolabelled against MCH (magenta) and orexin-A (blue). eYFP labeled cells did not stain for either orexin-A or MCH. B3) High magnification of boxed area in B2, arrows indicate ChR2-eYFP cell bodies. Scale: 100 μ m. C1–I1) eYFP immunoreactivity of ChR2-eYFP terminals in the VLPO, TMN, vPAG, LC, RTN (anterior; H1, posterior; I1) and PZ. Scale bar: 100 μ m. C2–F2: High magnification of boxed areas shown in panels to the right. Scale bar: 20 μ m. H2–I2: High magnification of dorsal boxed areas shown in H1 and I1.

Scale bar: 20 μm . H3–I3: High magnification of ventral boxed areas shown in H1 and I1. Scale bar: 20 μm . *Abbreviations: 3V; 3rd ventricle, 4V; 4th ventricle, 7N; facial nerve, aq; cerebral aqueduct, BSTS; bed nucleus of stria terminalis supracapsular part, cp; cerebellar peduncle, ec; external capsule, ic; internal capsule, fx; fornix, LC; locus coeruleus, LV; lateral ventricle, Me5; mesencephalic trigeminal nucleus, mt; mammillothalamic tract, opt; optic tract, ox; optic chiasm, PZ; parafacial zone, RTN; thalamic reticular nucleus, scp; superior cerebellar peduncle, VLPO; ventrolateral preoptic area, vPAG; ventral periaqueductal gray, vTMN; ventral tuberomammillary nucleus xscp; decussation of the superior cerebellar peduncle. See also Figure [S1].*

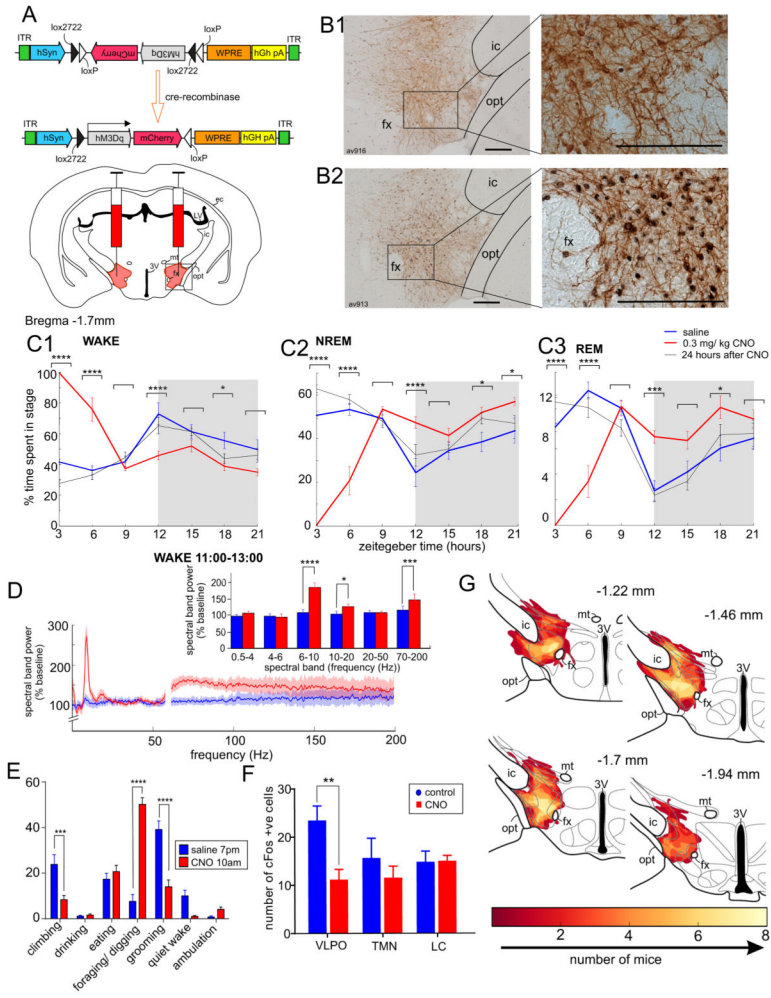


Figure 2. Conditional activation of LH VGAT+ neurons drives wakefulness

A) Schema of hM3Dq-mCherry construct and viral targeting to the LH of VGAT-ires-Cre mice. B) Dual immunolabeling against mCherry (brown) and c-Fos in LH VGAT+ cell bodies following injection of saline (B1) or CNO (B2) at 10AM, 90 minutes prior to sacrifice demonstrates that CNO activates neurons transduced with hM3Dq-mCherry, scale: 200µm. c) Percentage 3-hourly wake (C1), NREM sleep (C2) and REM sleep (C3) quantities following injection (n=8). Repeated measures 2-way ANOVA followed by Sidak post-hoc test. D) FFT analysis of wake during CNO activation (n=8), showing a ratio of power at each frequency post-injection compared with baseline. Shaded area indicates SEM. Inserts show averaged frequency bands. Repeated measures 2-way ANOVA followed by Sidak post-hoc test. E) Quantification of behaviors observed in mice during 1 hour following 10am CNO injection or 7pm saline injection. Bars represent the mean percent of time (± SEM) that mice (n=8) spent carrying out each behavior. 2-way ANOVA followed by Sidak post-hoc test. F) Quantification of c-Fos immunostaining in the VLPO, TMN and LC following saline injection at 10AM (n = 11) or CNO injection at 10AM (n = 12). Mean ± SEM shown. 2-way ANOVA followed by Sidak post-hoc test. G) Heat map showing overlapping regions of transfected neurons from mice in which unilateral LH VGAT+

activation increased wakefulness., * $p < 0.05$, ** $p < 0.01$, **** $p < 0.0001$, See also Figure [S2] and [S3]. *Abbreviations: 3V; 3rd ventricle, ec; external capsule, fx; fornix, LC; locus coeruleus, LH; lateral hypothalamus, mt; mammillothalamic tract, ic; internal capsule, opt; optic tract, TMN; tuberomammillary nucleus, VLPO; ventrolateral preoptic area.*

Author Manuscript

Author Manuscript

Author Manuscript

Author Manuscript

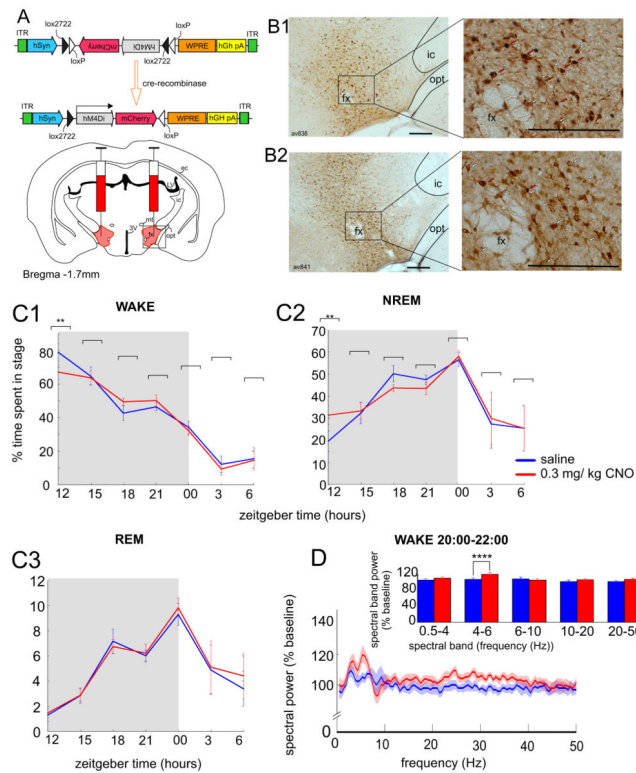


Figure 3. Conditional inhibition of LH VGAT+ neurons increases sleep

A) Schema of hM4Di-mCherry construct and viral targeting to the LH of VGAT-ires-Cre mice. B) Dual immunolabelling against mCherry (brown) and c-Fos in LH VGAT+ cell bodies following injection of saline (B1) or CNO (B2) at 7PM, 90 minutes prior to sacrifice. Red arrows show c-Fos and mCherry immunolabelled neurons, white arrows show neurons immunolabelled for mCherry only. CNO nearly eliminated c-Fos expression in LH VGAT+ neurons, indicating that they were inhibited, scale: 200 μ m. Percentage 3-hourly wake (C1), NREM sleep (C2) and REM sleep (C3) quantities following injection (n=9). Repeated measures 2-way ANOVA, followed by Sidak post-hoc test. d) FFT analysis of EEG During wake, showing the ratio of power at each frequency post-injection compared to baseline (n = 9). Shaded area indicates SEM. Inserts show averaged frequency bands. Repeated measures 2-way ANOVA, followed by Sidak post-hoc test, ** $p < 0.01$, **** $p < 0.0001$, R. Abbreviations: 3V; 3rd ventricle, ec; external capsule, fx; fornix, LH; lateral hypothalamus, mt; mammillothalamic tract, ic; internal capsule, opt; optic tract.